



## CAPABILITY ANALYSIS OF NONLINEAR 3D COARSE MESH FE MODELS IN REPRODUCING THE SHEAR CYCLIC RESPONSE OF RC MEMBERS

O. Arnau<sup>(1)</sup>, D. Murià-Vila<sup>(2)</sup>, K. Pérez<sup>(3)</sup> G. Zárate<sup>(4)</sup>

<sup>(1)</sup> Instituto de Ingeniería - Universidad Nacional Autónoma de México, [oriol@oriolarnau.com](mailto:oriol@oriolarnau.com)

<sup>(2)</sup> Instituto de Ingeniería - Universidad Nacional Autónoma de México, [dmv@pumas.ii.unam.mx](mailto:dmv@pumas.ii.unam.mx)

<sup>(3)</sup> Instituto de Ingeniería - Universidad Nacional Autónoma de México, [KPerezL@iingen.unam.mx](mailto:KPerezL@iingen.unam.mx)

<sup>(4)</sup> Instituto de Ingeniería - Universidad Nacional Autónoma de México, [GZarateG@iingen.unam.mx](mailto:GZarateG@iingen.unam.mx)

### **Abstract**

Present paper analyzes the capabilities of coarse mesh models in reproducing the nonlinear cyclic shear response of reinforced concrete members. Different finite elements types and mesh sizes are tested, determining the most optimal configurations in terms of precision-computational demand in order to be used for creating detailed models of buildings. In a first stage, solid and shell elements models are evaluated through the reproduction of the cyclic response of a coupling beam laboratory test reported in the bibliography. The influence of main modelling considerations and parameters like confinement, reinforcement adherence, and the influence of lateral cracking in compression strength is analyzed by comparing the overall response and energy dissipation. Most satisfactory modelling strategies and parameters are later used to reproduce the cyclic response of the complex wall-coupling beam system of the instrumented CCUT building. The influence of using different mesh type configurations, and of adopting different considerations for the main modelling parameters is also analyzed. Finally, conclusions about the achievable precision, limitations, modelling parameters influence, and best configurations for the use of coarse mesh models in reproducing the cyclic shear response of reinforced concrete members are presented and discussed.

*Keywords: Cyclic Shear response, Coarse mesh models, Coupling beams, Damage analysis, Nonlinear finite elements*



## 1. Introduction

The appropriate determination of the response presented by reinforced concrete (RC) damaged structures is a complex objective, which requires to adequately consider the complex phenomena occurred at both material and structural level. In this sense, finite elements modelling techniques (FE) have been constantly evolving along last decades in order to achieve a proper reproduction of actual response presented by concrete structures. On the other hand, they present a significant modelling and computational demand and, therefore, they are not usually considered when the structural analysis of complete buildings is intended. Beam and spring models are commonly used for such purpose, which simplifications define a low computational demand, but imply some drawbacks when complex geometries or shear dominant responses should be well reproduced.

Additionally, when trying to reproduce the dynamic response of a building it is necessary to account for the cyclic response of their structural members and connections. It takes a particular relevance in buildings in which energy dissipation is planned to be produced through the damage of RC structural members, which complex governing mechanisms, and the impossibility of testing all possible elements geometries, configurations, and materials, difficult an appropriate determination of the expected response. Therefore, it is of interest to determine techniques and strategies that allowed us to predict with a reasonable precision the cyclic response of RC structural members, and also to study the most appropriate and efficient way to incorporate them in buildings models.

In these sense, one of the most common RC members used to dissipate energy through its intended damage are the coupling beams, which are typically used to connect shear walls at story levels. When earthquake motions shake the building, coupling beams are subjected to alternate shear loads. Once motions are intense enough in order to exceed the linear response of the concrete, a stiffness degradation process occurs, dissipating energy through the hysteretic response presented by the coupling beam. Consequently, this response should be appropriately known and accounted for if the dynamic response of the building wants to be adequately reproduced. As presented in Sagaseta [1] and Belletti *et al.* [2], current modelling techniques based on cracking damage models allow to successfully reproduce the complex mechanisms governing the response of beams subjected to shear forces. Kwan and Billington [3] and Deaton [4] also show the capacity of advanced nonlinear FE models in reproducing the cyclic response of column-base and column-beam connections respectively.

As previously mentioned, nonlinear FE techniques require a high computational demand, thus limiting its use to single structural elements or connections [1-4]. Nowadays, the evolution of computers capabilities and the improvement of FE codes is opening the possibility of start modelling complete buildings in detail. Anyway, the majority of building cases would still require the use of a coarse mesh sizes in order to be viable from the computational cost point of view. Therefore, it is of paramount importance to determine which would be the most appropriate FE configurations to be used for RC buildings, and to evaluate their reliability. Pettersen [5] studied the response of 2D very large elements in reproducing the lateral monotonic response of a wall, concluding that used model succeed in predicting the stiffness of the wall, but failed in the ultimate load carrying capacity. For buildings, it would be interesting to study the capabilities of 3D models, for mesh sizes more according to buildings and current computational capacities, and in reproducing also the cyclic response.

Present paper initially analyzes the capabilities of coarse mesh models in reproducing the nonlinear cyclic shear response of RC members. For such purpose, the experiment performed by Naish [6] in a normally reinforced coupling beam is reproduced through 3D solid and shell elements models. Different mesh sizes are tested, and the influence of considering different modelling parameters like the compression confinement, the reinforcement adherence, and the reduction of compression strength due to lateral cracking is analyzed by comparing the overall response and energy dissipation. The most appropriate techniques and considerations are latter applied to reproduce the shear cyclic response of a wall-coupling beam section extracted from the seismically instrumented CCUT building in Mexico City. It presents a complex geometry due to E-shape walls and the fact that coupling beams run continuously by the inner side of the wall (Fig. 9). Solid and shell coarse mesh models results are compared to a more refined solids model, providing conclusions about the most suitable configuration for reproducing the response of the whole building.

## 2. Experimental test simulation

### 2.1 Test description

Naish [6] performed an experimental campaign in order to evaluate the cyclic response of coupling beams. Main objectives were focused on testing beams with materials and aspect ratios more according to the current construction tendency, to evaluate the impact of the floor slab, and to determine residual strengths and total plastic rotation capacities. The majority of the specimens were diagonally reinforced as current ACI standards indicate, but one specimen (FB33) presents a conventional reinforcement scheme (Fig.1), being selected as the reference case for this research since the CCUT beam-column intended to be reproduced at section 3 presents the same configuration (Fig.9).

The cyclic loading presented in Fig.1 was applied by means of a complex loading frame setup that aimed to ensure the zero rotation at the extreme of the specimen while maintaining constant zero axial force on the beam. First target displacements were achieved three consecutive times before being increased, reducing it to two and then to one for the last ones.

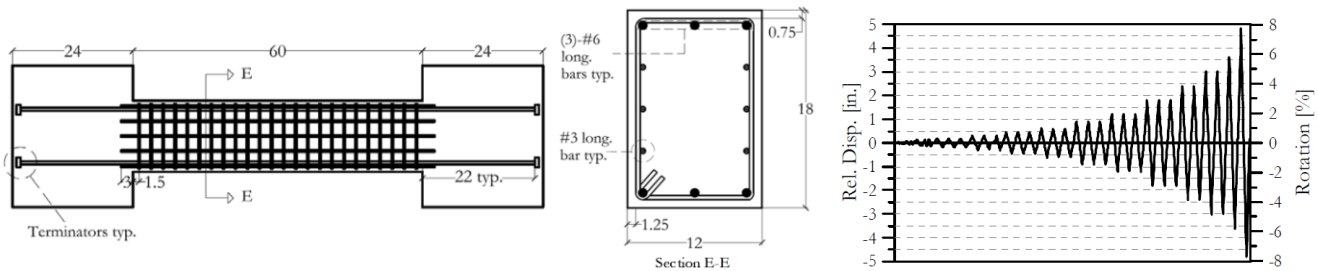


Fig. 1 – Dimensions and reinforcement of FB33 beam (in inches), and applied cyclic loading (Naish [6])

### 2.2 Models definition

With the aim of studying the different available possibilities of modelling the cyclic response of RC structures in a three-dimensional way, both solid and shell elements models are created. Two different mesh densities are tested for the solids, constructed with regular meshes on the base of representing the height of the coupling beam with 3 elements (SO-S1), or by using 5 elements (SO-S2) (Fig.2). Same scheme is adopted for shell models (SH-S1 and SH-S2), but also adding a more refined one (SH-S3) in which coupling beam height is modeled through 8 shell elements (Fig.2).

All models are created and analyzed following the recommendations presented in the complete RTD guidelines [7] for nonlinear finite element analysis of concrete structures, and in the user's manual of the employed software Diana 10 [8]. 20-node hexahedral elements with a 3x3x3 integration scheme are used for solid elements, whilst 8-node quadrilateral shell elements with also 3x3 integration in-plane and 3 integration points through elements' depth are used for shell elements. The RTD guidelines suggest the use of 7 out of plane integration points for shell elements, considering that this scheme is sufficient for capturing the gradual stiffness reduction caused by bending. In the present case, shell elements are used to study a plane response, thus reducing such proposal in order to improve the computational efficiency of the models. Both integration schemes are compared in a first stage in order to validate the assumed simplification.

The Total Strain Rotating Crack model included in Diana 10 software is used, as recommended by Deaton [4] and Kwan and Billington [3] for reproducing the shear and hysteretic response of RC members. Main material properties are obtained from Naish [6], NEES hub database [9], or derived from ACI-318-11 [10]. The inelastic response of concrete is considered as it is recommended in RTD guidelines [7]. A parabolic law is adopted for modelling the compressive response of concrete, whilst an exponential law is selected to reproduce the softening response presented after concrete cracking. Table 1 summarizes the adopted material properties and the correspondent source.

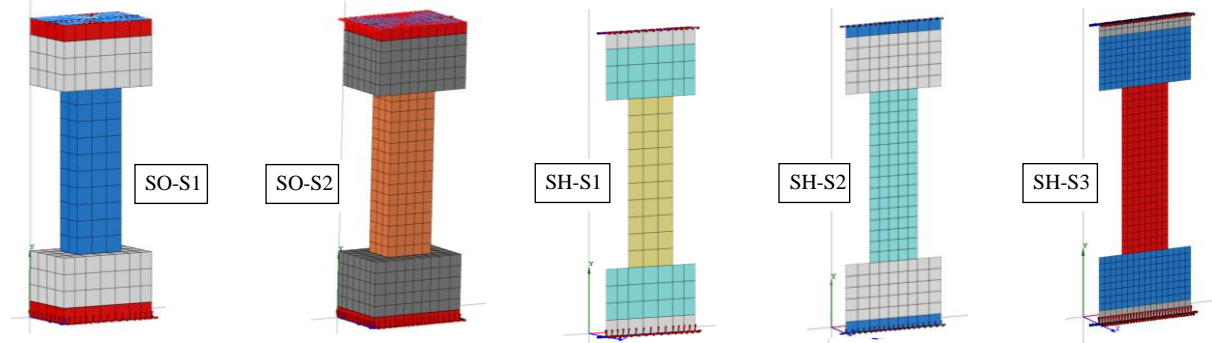


Fig. 2 – Solid and Shell models used in the present study

Table 1 – Mechanical properties adopted for constituent materials

Elements	Property	Nomenclature	Value		Source
			FB33	CCUT (21/28)	
Concrete	Modulus of elasticity	$E_c$ (N/mm <sup>2</sup> )	30442	13228 / 11456	ACI 318-11 [10]/ NTC [15]
	Poisson coefficient	$\nu_c$		0.15	RTD [7]
	Compression strength	$\sigma_{c,c}$ (N/mm <sup>2</sup> )	41.37	28.0 / 21.0	Naish [6] / CCUT Plans
	Comp. fracture energy	$G_C$ (N.mm/mm <sup>2</sup> )	22.9	18.4 / 15.8	RTD [7] (250- $G_F$ )
	Tensile strength	$\sigma_{t,c}$ (N/mm <sup>2</sup> )	4.0	2.01 / 1.74	ACI 318-11 [10] / NTC [15]
	Tensile fracture energy	$G_F$ (N.mm/mm <sup>2</sup> )	0.092	0.073 / 0.063	MC-90 [11] (d <sub>max</sub> =16)
Reinforcing	Modulus of elasticity	$E_s$ (N/mm <sup>2</sup> )		200000	Adopted
Steel	Poisson coefficient	$\nu_s$		0.3	Adopted
	Tensile yielding strength	$\sigma_{y,s}$ (N/mm <sup>2</sup> )	439 (#3) 483.5 (#6)	452.1 (#3-4) 449.0 (#8-10)	Naish NEES data [9] / Ochoa [17]
	Tensile ultimate strength	$\sigma_{u,s}$ (N/mm <sup>2</sup> )	679.1 (#3) 624.2 (#6)	729.5 (#3-4) 734.9 (#8-10)	Naish NEES data [9] / Ochoa [17]
	Tensile ultimate strain	$\epsilon_{u,s}$ (%)	25 (#3) 15.7 (#6)	14.2 (#3-4) 11.7 (#8-10)	Naish NEES data [9] / Ochoa [17]
	Concrete-Steel	Normal stiffness	$K_n$ (N/mm <sup>3</sup> )		2060
Interface	Tangential stiffness	$K_t$ (N/mm <sup>3</sup> )		206	From MC-90 curve [11]

The steel reinforcement is considered as embedded inside the concrete finite elements. Diana offers the possibility to account for the adherence response between both materials by automatically introducing interface elements. When using such option, Von Mises is the unique plasticity model available for reproducing the steel response, thus do not being able to accurately reproduce the cyclic response of the bars since the Bauschinger effect is not considered [4]. Therefore, a Von Misses plasticity model with kinematic hardening is adopted according to the Deaton [4] suggestions. The bond-slip response of the concrete-reinforcement interface is modelled through the cubic law option included in Diana 10 [8], adopting the maximum tangential stress ( $\tau_{\max} = 16.08$  N/mm<sup>2</sup>) and the relative displacement for its achievement ( $s_1 = 1$ mm) according to Model Code-90 [11] for good bond conditions. Bond slip reinforcements are only used for longitudinal reinforcements, whilst perfect bond conditions are adopted for the transversal reinforcement.

Similarly to the experimental configuration, the model is fixed in the bottom part. Rigid links are used in the vertical direction in order to warranty that no rotation is produced, but allowing the free vertical deformation since the experimental scheme is designed to produce null axial force on the beam. In order to avoid the possible cracking produced at the fixed edges due to the stiff boundary conditions, first top and bottom finite element rows are modelled with linear elastic material properties. The cyclic loading process is introduced by imposing horizontal displacements at the top part. The Secant BFGS iteration process is used, adopting an energy convergence criterion of 0.01%.

Table 2 presents the different modelling parameters tested in the models. The so called “Reference model” (Ref) include all the modelling features suggested in the RTD guidelines [7] for a proper reproduction of the nonlinear response of RC members. The unique exception is that in Ref model, the maximum reduction factor for considering the influence of the lateral cracking in the compression resistance is reduced to  $\beta_{min} = 0.6$  as suggested by the JSCE [12] for monotonic loading, because a better approach was found as it will be appraised in the next section. Notice but, that JSCE [12] proposes a subtraction of 0.2 to their values for cases where reversal cyclic loading could be repeated until a large tensile strain occurs, thus resulting in the same  $\beta_{min} = 0.4$  proposed by the RTD Guidelines [7]. The different modelling cases considered in the present study are defined by varying only one parameter at each time from the reference model, which description and nomenclature are listed in table 2 (right).

Table 2 – Different modelling considerations adopted in the study

Reference model description (REF)		Variations from REF model	
Considerations	Model in Diana 10 [8]	Name	Variation
Compression resistance reduction by lateral cracking.	Vecchio and Collins. Maximum reduction factor $\beta_{min} = 0.6$	RG	$\beta_{min} = 0.4$ (RTD [7])
		NLI	No lateral cracking influence
Concrete confinement	Selby and Vecchio	NC	Confinement is not considered
Poisson ratio reduction	Damage	NPD	Constant Poisson coefficient
Bond-Slip reinforcements	Cubic law, adapted from MC-90. Von Misses, kinematic plasticity.	FB	Perfectly bonded reinforcements
		MN	Perfectly bonded + Menegotto-Pinto model for the steel.

### 2.3 Analysis of results

Due to the difficulty of clearly apprising the results if different cycle responses are presented in the same graph, the obtained results are mainly compared through the force-displacement envelops and through energy dissipation diagrams.

The majority of the models presented convergence difficulties at some points during the collapse process. Anyway, calculations were continued despite the defined convergence criterion was not achieved at some steps, and dashed lines are used in order to indicate the response from the start of the numerical instabilities.

#### 2.3.1 Overall response

Fig.3 presents the envelop results obtained from the cyclic analysis of the different tested configurations for solid and shell size 2 meshes (left and right respectively). As can be observed for both models, the reference configuration (Ref) satisfactorily reproduce the overall response of the experiment, adequately fitting the deformational response (stiffness), the ultimate load, and for the solids model case, even a quite satisfactory following of the softening branch. Contrarily, the no consideration of the compression resistance reduction caused by lateral cracking (purple lines, NLI option) leads to an overestimation of the ultimate displacement, thus overestimating the actual ductility of the beam. On the other hand, when the maximum reduction in the compression stress by lateral cracking proposed by the RTD guidelines is adopted (RG option, green lines,  $\beta_{min} = 0.4$ , Table 2), the model predicts a premature failure. These results denote the significant influence of the compression response in the failure mechanism of the tested coupling beam.

Results also show that no significant influence is observed when the confinement formulation is deactivated for both solid and shell elements. It could indicate that no significant confinement effect influenced the actual response of the experimental beam due to the low amount of transversal reinforcement, moreover when numerical results adequately reproduce the experimental response without confinement considerations. Shell elements cannot even consider the reinforcement transversally placed to the elements, thus do not being able to reproduce the reinforcement restraining in transversal direction. Further studies should be performed on

elements presenting a higher amount of transversal reinforcement in order to clarify the numerical influence of the confinement model. The no consideration of the Poisson coefficient damage also does not show a significant influence in the average response, despite a higher deformation is achieved in the negative loading branch for the shell model (but it is not fully converged). As denoted by dashed lines in Fig.3, in general terms numerical instabilities start with the failure initiation of the specimen. Solid elements models present a higher stability in this part, achieving a better reproduction of the softening branch for a higher number of cases.

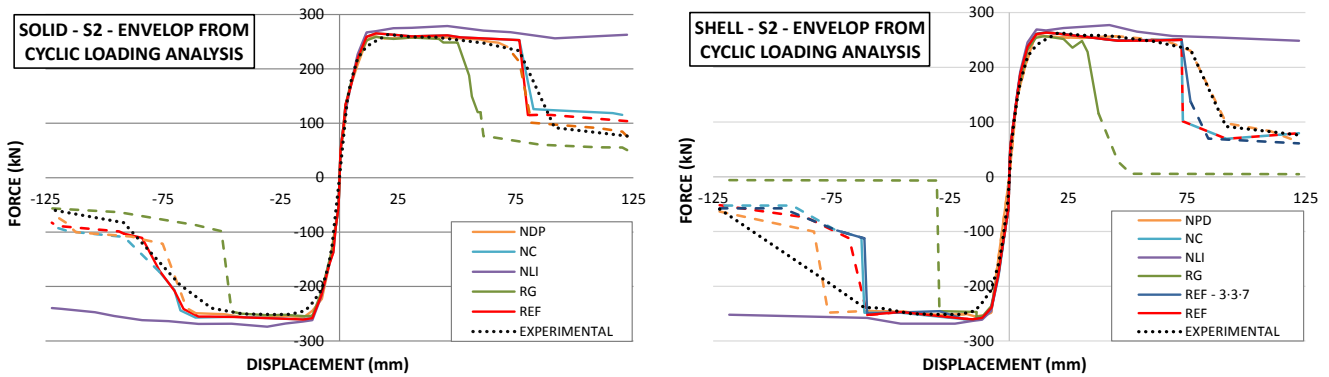


Fig. 3 – Overall response of different modelling options using size 2 solids (left) and shells (right)

In general terms, solid elements and shell elements models in size 2 meshes provided very similar results. The use of the 3-3-3 or 3-3-7 integration scheme for shell elements (Fig.3, right), does not provide significant differences in the reference case.

### 2.3.2 Cyclic response and energy dissipation

Fig.4 presents the cyclic response obtained for size 2 solid and shell models (left and right respectively). As it was mentioned in the previous section, both present a good agreement in ultimate load and displacement prediction. Nevertheless, different loading and unloading paths are presented along last cycles. Both models provide a very similar and accurate response up to cycles 8 – 9 (maximum displacement around 30mm) (Fig. 5). From that point, solid model tends to overestimate the reloading branch, whilst shell model tends to show a significant pinching in its hysteretic response (view cycle 11, Fig.5). As a consequence, the energy dissipation predicted by solid model for cycles 10 to 12 is significantly higher than the one experimentally obtained, as shown in Fig.6 (two last cycles 13-14, have not been considered in the energy dissipation analysis since it is considered that the structure has already failed). The energy dissipation predicted by shell model at these cycles is much more accurate because the pinching phenomenon is compensated by an unrealistic compression stiffness that produce similar areas inside the hysteretic loops.

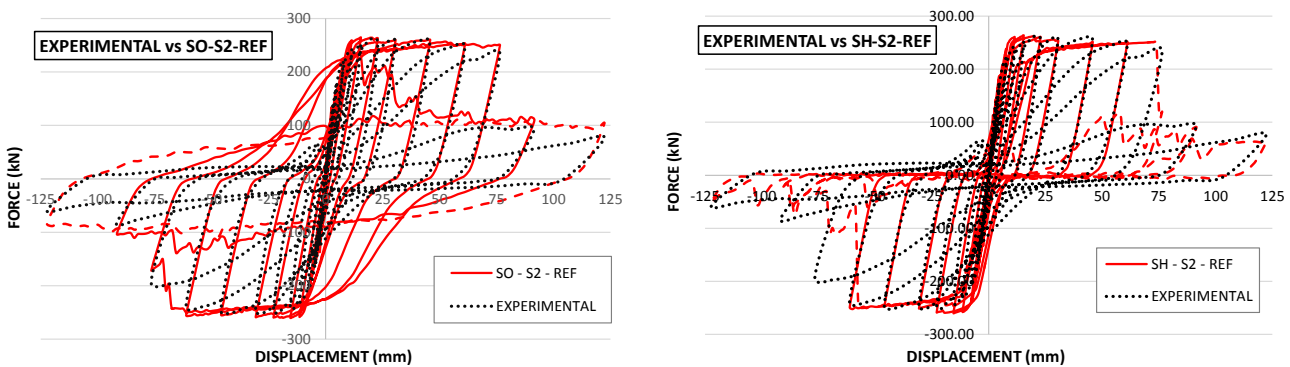


Fig. 4 – Cyclic response of reference models using size 2 solids (left) and shells (right)

On the other hand, the energy dissipation per cycle of both models is quite accurate for the main dissipation loops (cycles 6-7 to 9), where relative displacements from 10 to 30mm are covered. Initial loops (cycles 2-3), also show a very good agreement despite the small amount of energy dissipated. Out of the last

cycles, the worst prediction is found at 4 to 5-6 cycles, where models tend to underestimate the energy dissipation despite the obtained maximum load and displacement satisfactorily fits the experimental results. This fact can be also observed when analyzing the accumulated dissipated energy, where the numerical results slightly differ from the experimental ones. Despite that, a quite satisfactory agreement can be observed in the overall energy dissipation provided by both numerical models.

Fig.6 also shows how the main modelling parameters do not significantly influence the obtained energy dissipation process along the middle cycles, out of the premature or longer ruptures provided by RG or NLI models. Otherwise, the no consideration of the Poisson coefficient damage (NPD) provides an underestimation of the dissipated energy for middle cycles, but tends to provide more accurate prediction for last cycles.

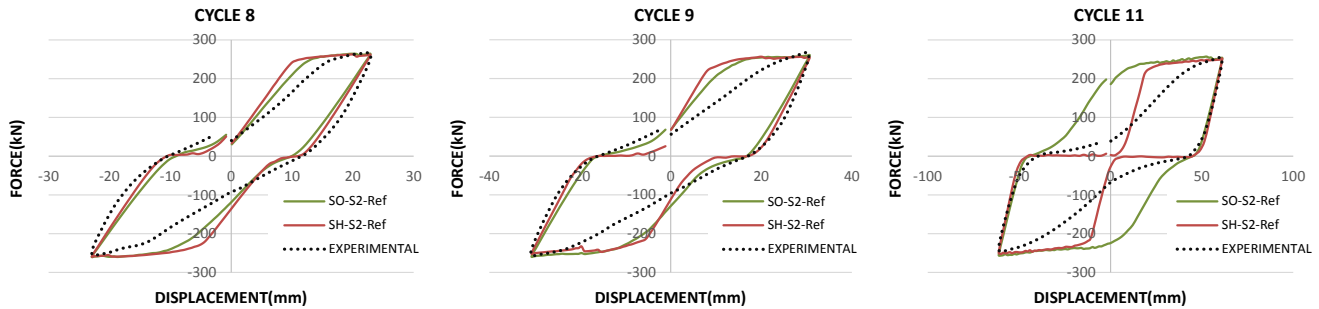


Fig. 5 – Hysteretic response of reference size 2 models at different loading cycles

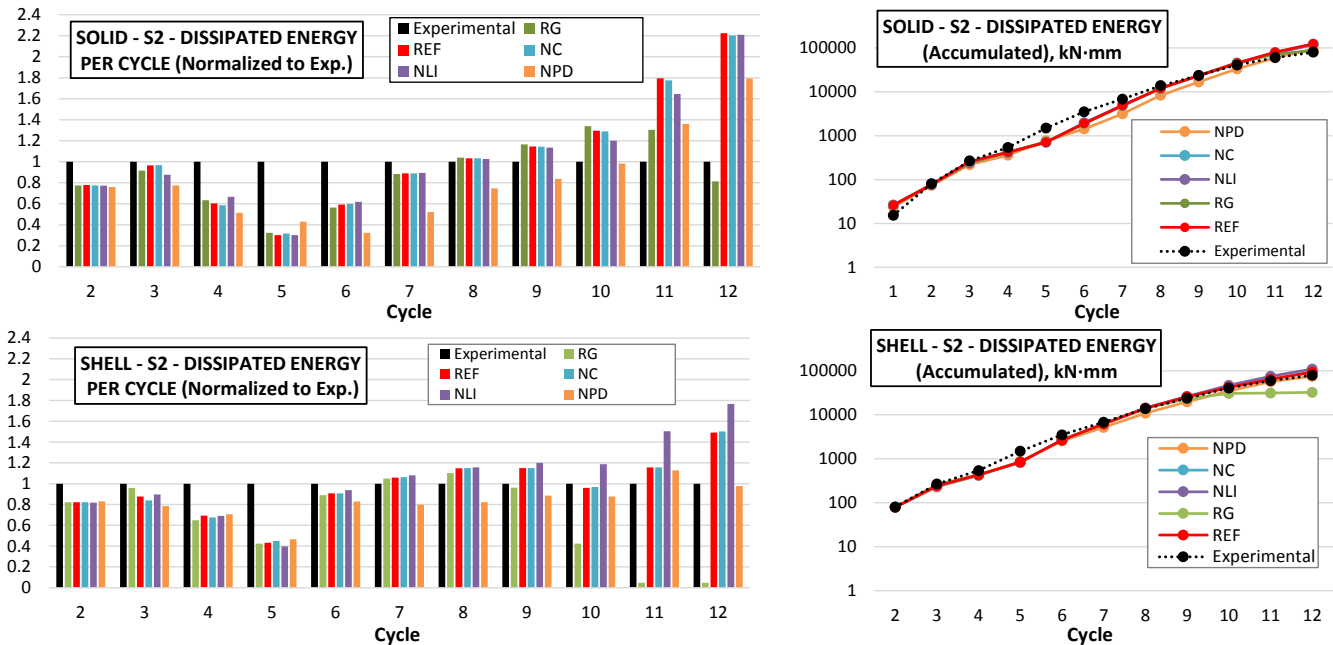


Fig. 6 – Energy dissipation for different modelling considerations of size 2 mesh models

### 2.3.3 Mesh size influence

Fig.7 presents the results obtained for different mesh sizes when the reference considerations are used. As can be observed, no significant difference is presented between the solid elements meshes (SO-S1 and SO-S2) in both terms of general response (envelop from cyclic loading) and energy dissipation. Therefore, and for computational economy, it would be recommended to use size 1 mesh (where the height of the beam is divided in 3 elements, Fig.2) when solid elements are employed to reproduce the response of coupling beams. On the contrary, when shell elements are employed, size 1 mesh is not able to adequately reproduce the actual response, providing larger ultimate displacements since the local mechanism at the corners are not reproduced with enough

precision. Size 3 shell mesh, shows the same results as size 2 and a good agreement to the experimental results at one side of the envelop results, but a slight premature failure is predicted at the other side. As can be observed in Fig.7 left, this failure is displayed with dashed lines denoting that convergence criterion was not completely achieved at that part, thus being necessary to take some reserves about the significance of this ultimate cycles results. However, size 3 shell mesh provides a better approach to the actual energy dissipation at middle cycles 4 to 6.

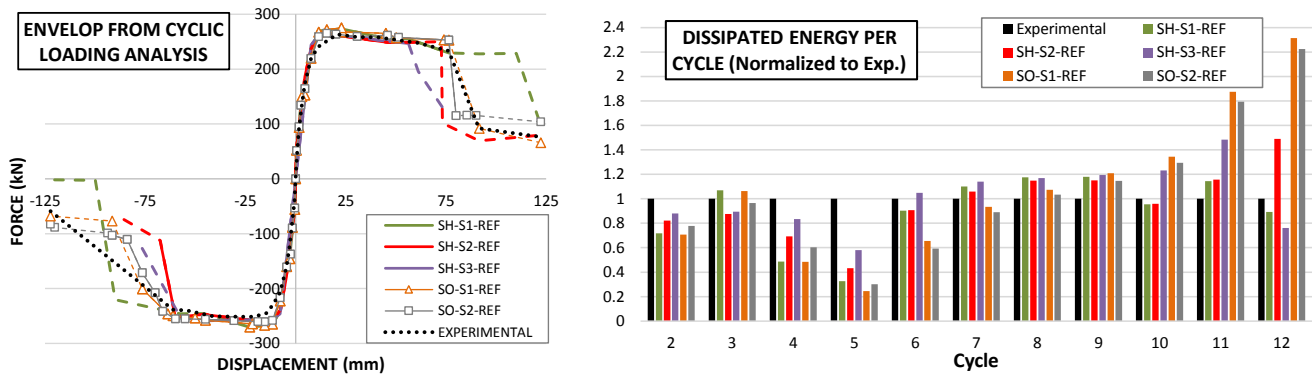


Fig. 7 – Comparison of mesh size influence

### 2.3.4 Bond-Slip influence

Fig.8 shows the influence of not considering the bond-slip in the reinforcement through 2 different material models: the same Von Mises plasticity model with kinematic hardening (FB, Table 2), and a Menegotto-Pinto model (MN). This last model allows to reproduce in a more accurate way the actual hysteretic response of the reinforcing steel, since it considers the Bauschinger effect [3-4]. Due to the lack of knowledge about the actual cyclic response exhibit by the reinforcement used in the test, the parameters for the Menegotto-Pinto model are assumed from Yu [13]. As can be observed, the overall response provided by the full bond model (FB) is very close to the one obtained in the reference model, whilst the Menegotto-Pinto Model provided a higher ultimate force at a lower displacement. It could be caused by the isotropic hardening component of the response included in the bibliographic data adopted for the model, instead of the kinematic hardening option adopted in the Von Mises models.

As shown in Fig.8 right, perfectly bonded reinforcements provide a bad approximation of the energy dissipated at initial cycles 3 to 5, where they also show an overestimation of the stiffness and of the pinching response. For middle cycles, FB model shows a small overestimation of the dissipated energy whilst MN model approaches a little bit better the reference model and the experimental results. Anyway, both results stay in a range of difference between 10 and 20% of energy dissipation for significant cycles, and its use could be of interest for huge models in front of high displacement demands due to the computation savings obtained from avoiding the interface elements that reproduce the bond-slip.

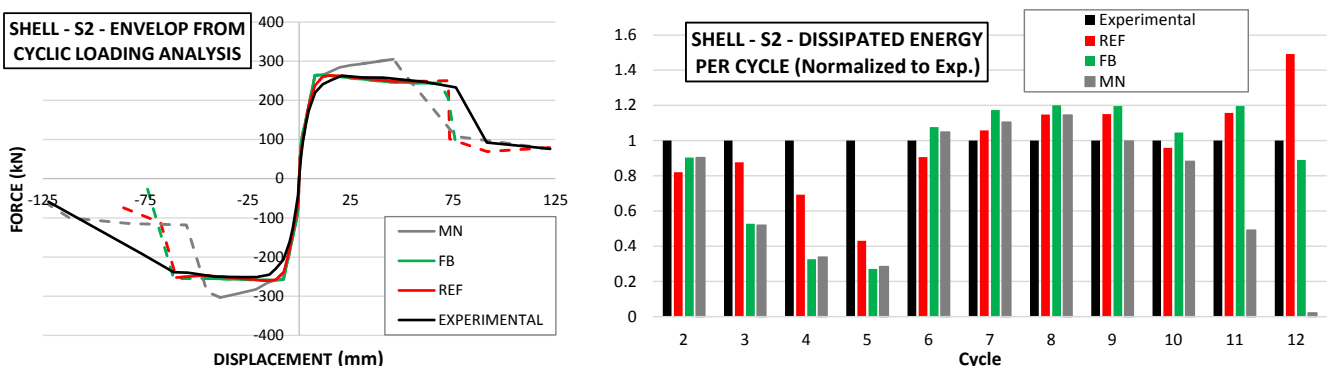


Fig. 8 – Comparison of results obtained with fully bonded reinforcements

### 3. CCUT wall - coupling beam system

#### 3.1 Geometrical and material description

The present section aims to reproduce the structural response presented by the complex wall-coupling beam of the CCUT building. The CCUT complex consists of a 22-storey tower and three low-rise structures located at Mexico City. The RC tower was damaged during Mexico’s 85 earthquake, and recently has been retrofitted and monitored [14]. As shown in Fig.9, the wall-coupling beam system presents a complex geometry due to the combination of columns and thin walls defining an E-shape wall, and the coupling beam continuously ran by the inner side. The particular configuration of sizes and reinforcements presented in Fig.9 corresponds to stories 11 to 15, where different concrete compressive strengths of 21 and 28 N/mm<sup>2</sup> were employed for beam and wall respectively. According to the usual practice during the construction years in the zone, it is assumed that concrete with low specific weight (due to andesite aggregate) was used. As a consequence, the low stiffness modulus presented at Table 1 are obtained from applying the local code NTC-DF-2004 [15] for class 2 concretes. The response of the original wall-coupling beam configuration is studied in this section, thus not considering the carbon fiber sheets recently added to some beams during the retrofitting process.

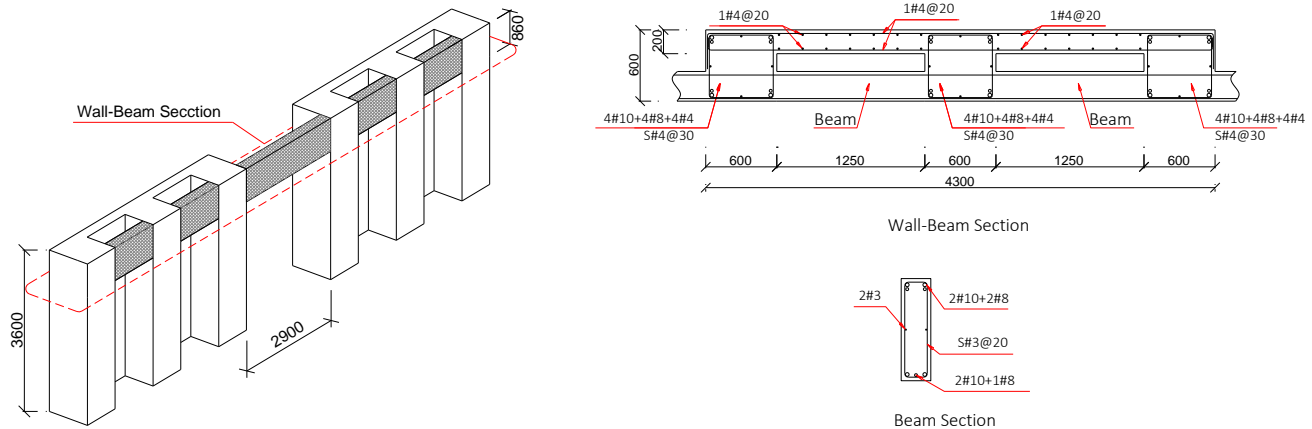


Fig. 9 – Detailing of the considered CCUT wall-coupling beam (in mm)

#### 3.2 Models definition

Modelling techniques exposed along section 2 are here used in order to define the three different models shown in Fig.10, which consider the half height of the wall at each side of the coupling beam. The mesh sizes obtained as the most efficient ones in previous section (size 1 for solids and size 2 for shells) are compared with the results obtained by the size 2 solid elements mesh. In the shell elements model (SH-S2), the width of the column is assigned to the beam elements placed in the connection zone (orange elements in Fig.10) in order to create a more realistic stiffness change in the beam. Same numerical strategies defined along section 2 are here employed, adopting the particular material values listed at Table 1. Just mention that thin wall reinforcement was considered as grid reinforcement in Diana 10 [8], thus being distributed in a 2D plane and perfectly bonded to the elements. First top and bottom elements rows are considered as elastic in order to avoid local cracking derived from the stiff boundaries.

Vertical displacement is introduced at the base of the left wall, whilst the right wall remains restrained at his bottom. Rigid connections are applied at the top of each wall in order to guarantee that no rotation is produced. Left wall is not restrained in horizontal direction and, therefore, no compression is introduced in the beam. The cyclic loading is applied by imposing vertical displacement cycles of 10, 20, 30, 40, 50 and 60mm towards both sides. The same analysis conditions of iteration procedure and convergence criterion exposed in section 2 are used.

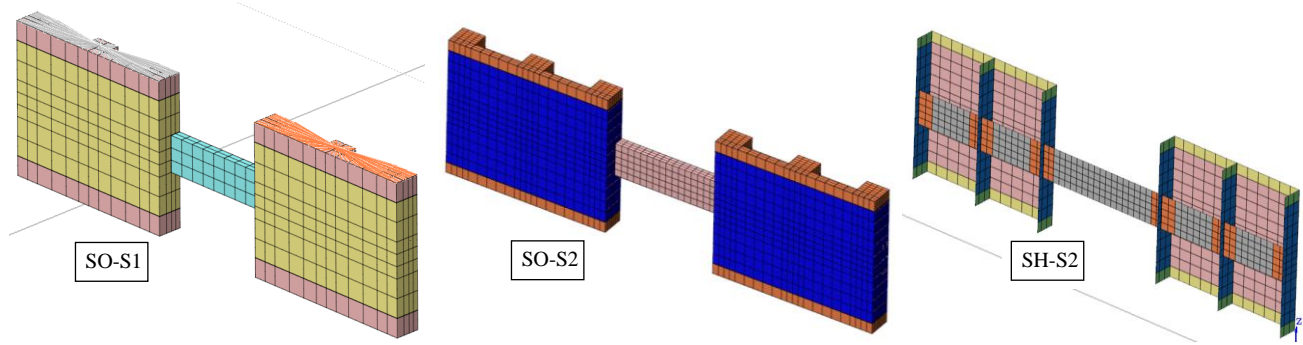


Fig. 10 – Solid and Shell models of the CCUT wall-coupling beam system

### 3.3 Analysis of results

Fig.11 left presents the results obtained for the three different tested meshes. As can be observed, the general response of the system presents failure a low ductility, do not achieving the plastic response presented by the coupling beam of section 2. As a consequence, only four of the six defined cycles were completed, achieving a maximum relative displacement of 40mm. Results seem to indicate that response is controlled by a diagonal tension failure prior to establish a flexural hinging, as described by Ihtiyar and Breña [16] for coupling beams with low transverse reinforcement. Therefore, a fragile response should be expected at low ductility levels for the original CCUT wall-coupling beam system, thus enhancing the significance of the carbon fiber sheets placed at some of them during the retrofitting process.

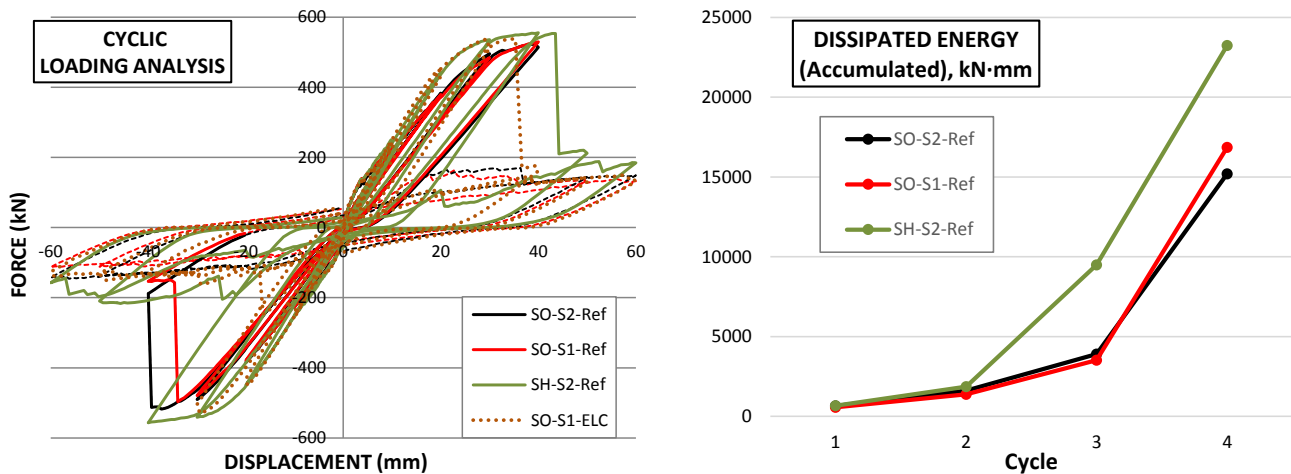


Fig. 11 – CCUT wall-beam cyclic response and energy dissipation for reference models

No significant differences are presented between the cyclic responses of the two solid elements models (Fig. 11), confirming the good capabilities of the proposed coarse mesh SO-S1 also observed in previous section. Otherwise, shell elements model provides a stiffer response, achieving a slightly higher ultimate load (6.3%). This response difference is caused by the fact that the configuration used in shell model, with column elements placed in transversal direction to beams, is not able to reproduce the local damage emerged at the column (Fig.12 right). This hypothesis is confirmed when a solid mesh S1 model is calculated by considering linear elastic properties for the columns, obtaining results similar to the shell model (SO-S1-ELC, Fig.11 left). The originated different response produce a higher energy dissipation when the shell model is used (Fig.11 right). Probably, and according to the results obtained in section 2, if columns were modelled in the longitudinal direction of the beam, the local response could have been reproduced in a more appropriate manner, and more accurate results would be achieved for this particular analysis. On the other hand, resolution would be lost in the column response in transversal direction, which could also be important for the building response. Therefore, the limitations of the shell elements should be taken into account in order to decide their best geometrical configuration according to the most relevant response to reproduce.

Fig.12 shows the envelop response obtained when the different modelling considerations listed in Table 2 are applied to the size 1 solid mesh model. In the same way observed in section 2, the no consideration of the confinement effects (NC) does not produce significant differences in the response. The causes could be the same already presented, but also adding the fact that in this coupling beam, failure seems to be produced by diagonal tension, thus even diminishing the influence of the compressive behavior in the response. In the same sense, a greater reduction in the compressive strength due to lateral cracking (RG option, green lines,  $\beta_{min} = 0.4$ , Table 2), does not produce the significant difference in premature failure observed for coupling beam of section 2, also supporting the idea that compression response in this case is not as relevant as in the previous section case. The no consideration of the lateral cracking influence (NLI) also provides a higher failure displacement, achieving to complete the whole 6 cycles. The no consideration of the Poisson coefficient damage (NPD) leads to a less stiff response, probably denoting the overestimation in the transversal strains that a constant Poisson coefficient can produce in total strain crack formulations [1], that in this case are not properly restrained by the low transversal reinforcement ratio. Consequently, the plastic response is produced before achieving the ultimate load, thus being able to also complete all the imposed cycles.

The consideration of perfect bond between the reinforcement and the concrete leads to a good stiffness response, but a clear premature failure (FB in Fig.12). This fact contradicts the observations performed in section 2, where the full bond reinforcement practically exhibits the same results obtained for the bond-slip option. Therefore, the influence of the different modelling parameters and considerations would depend on the main mechanisms governing the response and the failure of the element. It would be necessary to appropriately determine them, and focus more efforts in accurately reproduce the materials or phenomena that could play the most significant influence on the structure response.

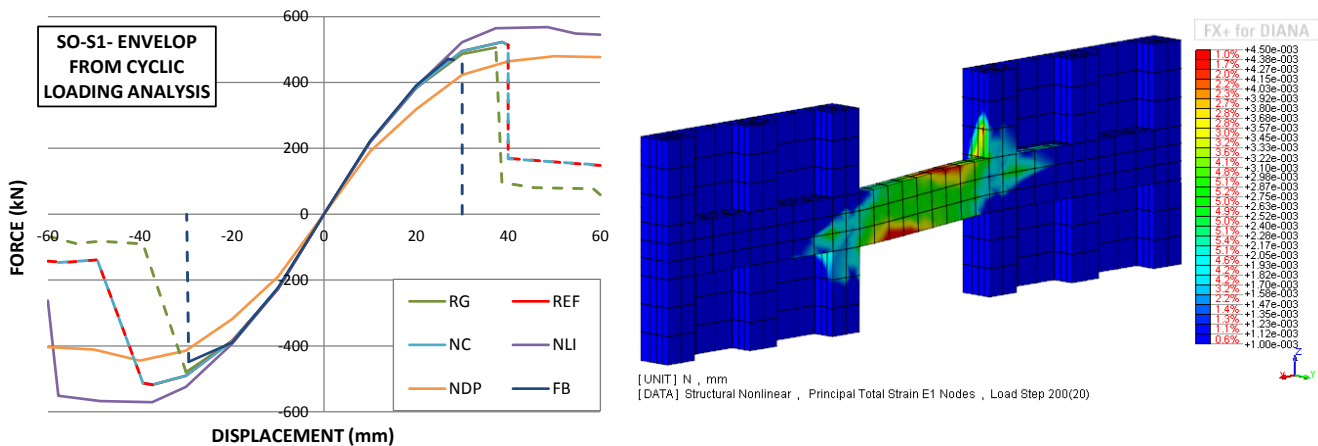


Fig. 12 – Influence of main modelling parameters in CCUT wall-beam response (left), and principal tensile strain (indicative of damage) occurred at beam and column for 20mm of displacement (SO-S1-Ref) (right)

#### 4. Conclusions

The shear cyclic response of coupling beams has been successfully reproduced through the use of both solid and shell coarse mesh finite elements models. For solid type, a regular mesh of 20-node hexahedron elements dividing the height and the thickness in 3 and 2 elements respectively, can provide a satisfactory approximation to the actual response. When using 8-node quadrilateral shell elements, it is necessary to divide the height of the beam in more elements, obtaining satisfactory results with 5 in the present study. Both configurations present a relatively low computation cost, thus emerging as a powerful tool in order to reproduce the response of a whole building governed by coupling beams.

Additionally, the presented methodologies can also be used in order to determine the hysteretic response of particular sections of a structure. They allowed to analyze the cyclic response of the complex wall-coupling beam system originally presented at the CCUT building, opening the possibility to numerically study the most



appropriate design and retrofitting techniques for similar RC members. The obtained characterization of the cyclic response can then be used in order to define more simplified models of buildings.

The influence presented by different modelling parameters or considerations in the numerically obtained results depends on the structural response of the reproduced element, and on their main governing mechanisms. Therefore, special attention should be provided in determining the most influence parameters or phenomena according to the structural response, and focus the efforts in accurately reproduce them.

Shell elements models allowed to provide accurate results in modelling the complex response of the analyzed coupling beams with a low computation demand. However, their limitations in the transverse direction, of no considering reinforcements orthogonally placed to the elements surface, and in reproducing local 3D responses like the ones occurred in the wall-beam connection, have been pointed out. Consequently, these limitations have to be taken into account when deciding the model configuration, trying to achieve the geometry of the structure by placing the shell elements according to the most relevant response to reproduce.

## 5. References

- [1] Sagaseta J (2008): The influence of aggregate fracture on the shear strength of reinforced concrete beams. Ph.D. Thesis, Imperial College London.
- [2] Belletti B, Damoni C, Uijl JA, Hendriks M, Walraven JC (2013): Shear resistance evaluation for prestressed concrete bridge beams: fib Model Code 2010 guidelines for level IV approximations. *Structural Concrete*, **14** (3), 242-248.
- [3] Kwan WP, Billington SL (2001): Simulation of structural concrete under cyclic load. *Journal of Structural Engineering*, **127** (12), 1391-1401.
- [4] Deaton JB (2013): Nonlinear finite element analysis of reinforced concrete exterior beam-column joints with nonseismic detailing. Ph.D. Thesis, Georgia Institute of Technology.
- [5] Pettersen JS (2014): Non-Linear finite element analyses of reinforced concrete with large scale elements. Ms.C. Thesis, Norwegian University of Science and Technology – Trondheim.
- [6] Naish DAB (2010): Testing and modeling of reinforced concrete coupling beams. Ph.D. Thesis, University of California, Los Angeles.
- [7] Rijkswaterstaat Centre for Infrastructure (2012): Guidelines for nonlinear finite element analyses of concrete structures. RTD:1016:2012.
- [8] TNO Diana (2016): Diana user's manual. Release 10.0
- [9] NEES Hub. Data from Naish tests. <https://nees.org/warehouse/experiments/1100>
- [10] ACI Committee 318 (2011): Building Code Requirements for Structural Concrete (ACI 318-11). ACI.
- [11] CEB-FIP (1993): CEB-FIP Model Code 1990. Thomas Telford, London.
- [12] JSCE (2010): JSCE Guidelines for Concrete No. 15: Standard Specifications for Concrete Structures - 2007 "Design". Tech. rep., Japan Society of Civil Engineers.
- [13] Yu W (2006): Inelastic modeling of reinforcing bars and blind analysis of the benchmark tests on beam-column joints under cyclic loading. Master Thesis, Università degli Studi di Pavia.
- [14] Murià-Vila D, Camargo J, Aldama BD, Rodríguez G, Aguilar LA, Ayala M (2013): Structural health monitoring of an instrumented building in Mexico with accelerometers and GPS sensors. *6<sup>th</sup> International Conference on Structural Health Monitoring of Intelligent Infrastructure*, Hong Kong.
- [15] NTC-DF (2004): Normas Técnicas Complementarias del Reglamento de Construcciones para el Distrito Federal. Administración Pública del Distrito Federal. México.(in Spanish)
- [16] Ihtiyar O, Breña SF (2007): Assessment of FEMA 356 techniques for orthogonally reinforced coupling beams through experimental testing. *Structural engineering research Frontiers, ASCE structural congress 2007*, Long Beach, USA.
- [17] Ochoa OA (2015): Calibración de un modelo no lineal tridimensional de un edificio instrumentado. Ms.C. Thesis, Institute of Engineering, National Autonomous University of Mexico. (in Spanish)